



# OPEN Impact of optimized and conventional facility designs on outpatient abdominal MRI workflow efficiency

Alexander Herold<sup>1,2</sup>, Leo L. Tsai<sup>1</sup>, Wei-Ching Lo<sup>3</sup>, Azadeh Tabari<sup>1</sup>, Barbara D. Wichtmann<sup>1,4</sup>, Andrew Sharp<sup>1</sup>, Bryan Clifford<sup>3</sup>, Min Lang<sup>1</sup>, Sean P. Hartman<sup>1</sup>, Lauren M. Melski<sup>1</sup>, Majeed Waqas<sup>3</sup>, Michael Weber<sup>2</sup>, Oleg Pianykh<sup>1</sup>, Susie Y. Huang<sup>1</sup>, Mukesh G. Harisinghani<sup>1</sup> & Onofrio A. Catalano<sup>1,2</sup>

**Purpose:** The goal of this study was to evaluate the outpatient workflow efficiency of an optimized facility (OF) compared to an established reference facility (RF) for abdominal magnetic resonance imaging (MRI). **Methods:** In this retrospective study, we analyzed 2,723 contrast-enhanced liver and prostate MRI examinations conducted between March 2022 and April 2024. All examinations were performed on 3T scanners (MAGNETOM Vida, Siemens Healthineers) at two different imaging facilities within our institution. The optimized facility featured a three-bay setup, with each bay consisting of one magnet, two dockable tables, and one dedicated preparation room, while the reference facility utilized a single scanner-single table setup with one dedicated preparation room. Workflow metrics were extracted from scanner logs and electronic health records. Three-way ANOVA and chi-square tests were used to assess the impact of facility design, body region, and date on workflow metrics. **Results:** The OF significantly reduced mean table turnaround times (4.6 min vs. 8.3 min,  $p < 0.001$ ) and achieved shorter total process cycle times for both liver (30.6 min vs. 32.7 min,  $p < 0.01$ ) and prostate exams (32.5 min vs. 36.4 min,  $p < 0.001$ ) compared to the RF. Additionally, the OF achieved turnaround times of  $\leq 1$  min in 37.2% of exams, compared to just 0.6% at the RF ( $p < 0.001$ ). On-time performance was also notably higher at the OF (79.4% vs. 66.0%,  $p < 0.001$ ). Furthermore, the mean time from patient arrival to exam start was reduced by 9 min at the OF ( $p < 0.001$ ). Minor differences in acquisition times were observed between facilities, with both benefiting from deep learning reconstruction techniques. **Conclusion:** The optimized MRI facility demonstrated superior outpatient workflow efficiency compared to an already efficient reference facility, particularly in table turnover time, resulting in increased patient throughput for abdominal MRI examinations. These findings highlight that even highly efficient MRI facilities can significantly benefit from comprehensive redesign strategies.

**Keywords** Abdominal MRI, Workflow optimization, Turnaround time, Dockable tables, Deep learning

Over the past few decades, the demand for abdominal MRI scans has steadily grown as it has become an essential tool for lesion characterization, diagnosing and staging diseases, and assessing treatment response. For example, several studies have focused on the recent surge in pre-biopsy prostate MRI exams across different populations and stages of evaluation<sup>1,2</sup>. Similarly, liver MRI has emerged as the modality of choice for the evaluation of patients with focal or diffuse liver diseases<sup>3</sup>. While MRI offers distinct advantages, including lack of radiation exposure and high diagnostic accuracy, it also presents challenges, in particular relatively longer scan times compared to computed tomography or ultrasonography. Lengthy examination times, often necessitated by the

<sup>1</sup>Department of Radiology, Massachusetts General Hospital, Harvard University Medical School, Boston, MA, USA. <sup>2</sup>Department of Biomedical Imaging and Image-Guided Therapy, Medical University of Vienna, Vienna, Austria. <sup>3</sup>Siemens Medical Solutions USA, Boston, MA, USA. <sup>4</sup>Department of Neuroradiology, University Hospital Bonn, Bonn, Germany. <sup>5</sup>Division of Abdominal Imaging, Department of Radiology, Massachusetts General Hospital, Harvard Medical School, 55 Fruit Street, White Building, Room 270, Boston, MA 02114, USA. ✉email: ocatalano@mgh.harvard.edu

complexity of multiparametric protocols, can limit clinical applicability and strain workflow efficiency, especially in the face of growing clinical demand. This results in significant pressure on healthcare systems to optimize MRI utilization while maintaining patient access and imaging quality.

While abbreviated MRI protocols<sup>4</sup> as well as technological advancements, including acceleration techniques such as compressed sensing<sup>5</sup>, parallel imaging<sup>6</sup> and deep learning reconstruction methods<sup>7</sup>, have focused on reducing scan time, i.e. acquisition time, in abdominal MRI imaging, the non-acquisition time, particularly patient preparation and table turnaround time, represent substantial opportunities for workflow optimization.

Non-acquisition time components can account for a substantial portion of the total process cycle<sup>8</sup> and often become rate-limiting steps in the MRI workflow. Conventional MRI setups, where patient positioning and preparation occur directly in the scanner room, are prone to workflow delays that can cascade into subsequent appointments, affecting overall efficiency as well as patient experience. To address these challenges, some institutions have recently implemented innovative designs such as dockable tables and dedicated preparation bays, aiming to reduce turnaround times between examinations<sup>9</sup>. By adopting such approaches, healthcare providers can enhance the value of MRI services through increased patient throughput without compromising exam quality or patient care.

In our institution, the majority of abdominal MRI exams, including liver and prostate scans, are performed at two imaging facilities: a well-established, efficient outpatient facility with a conventional MRI scanner setup and a new outpatient MRI facility that opened in March 2022. The new facility incorporates innovative design elements such as dual swappable tables for each magnet, aimed at improving operational efficiency and patient experience.

The aim of this study was to compare this new, optimized facility (OF) with our established reference facility (RF), focusing particularly on the impact of the innovative design elements implemented at the OF. We hypothesized that the optimization efforts at OF would result in reduced table turnaround times, increased patient throughput, shorter times from patient arrival to the start of the exam and improved on-time performance compared to the already efficient RF. Additionally, we analyzed the impact of deep learning (DL) techniques on acquisition time at both facilities.

## Materials and methods

### Patient cohort

This retrospective study included patients who underwent routine contrast-enhanced MRI examinations of the liver or prostate as part of their standard clinical care between March 2022 and April 2024. The study was approved by the Mass General Brigham Institutional Review Board (IRB). All methods were performed in accordance with the relevant institutional guidelines and regulations. Due to the retrospective nature of the study, the Mass General Brigham IRB waived the requirement for informed consent. The following exclusion criteria were applied: age < 18 years, hepatospecific contrast-enhanced studies, incomplete examinations, scanning of multiple body regions in one exam (including MRCP), and incomplete data extraction from the scanner log. After applying these criteria, we excluded a total of 650 examinations: 52 exams due to age < 18 years, 45 exams for hepatospecific contrast-enhanced studies, 58 exams for incomplete examinations, 473 exams for scanning multiple body regions (including MRCP), and 22 exams due to incomplete data extraction from the scanner log. This left 2,723 MRI examinations included in the final analysis.

### MRI facilities

All examinations were acquired on 3T MRI scanners (MAGNETOM Vida, Siemens Healthineers, Forchheim, Germany) at two abdominal MRI facilities within our hospital network: one established outpatient reference facility and a new, optimized MRI facility. The RF is a highly efficient, multi-modality imaging center that employs a traditional MRI scanner setup with a single, fixed scanning table and one preparation bay. Adjacent to the scanner suite, a designated area for peripheral intravenous line placement by nursing staff enables streamlined patient preparation. However, this arrangement required sequential patient processing, with the next patient waiting until the current exam was completed before entering the scanner room for preparation. In contrast, the OF, which began operations in March 2022, is an exclusive MRI facility featuring an innovative layout designed to enhance efficiency and patient throughput. It includes three MRI scanners and three dedicated preparation bays. Each scanner is equipped with a pair of interchangeable dockable tables with a corresponding duplicate set of coils. The patient preparation bays are positioned in a direct path to the scanner, separated by a central corridor and are used for patient positioning, intravenous catheter placement, coil and earplugs/headphone placement, allowing for concurrent patient preparation and scanning. Once the preceding exam was completed, the tables were swapped immediately, enabling a seamless transition between patients and minimizing congestion. Additionally, the MRI scanners are each angulated to facilitate a faster docking process. A detailed floorplan of the new imaging facility was published previously by Lang et al.<sup>10</sup>. This innovative design allowed for a reduction in slot times from 45 min at RF to 30 min at OF.

Both facilities maintained standardized staffing levels with two MRI technologists per scanner. The optimized facility additionally employed one technologist aide shared across all three scanners to support the parallel workflow enabled by the preparation bay and dockable table system. The aide assisted with patient transport and preparation tasks, allowing technologists to focus on scanning procedures.

### Image acquisition

Image acquisition at both facilities was performed using identical protocols implemented across institutions. The liver protocol consisted of Dixon T1-weighted imaging yielding in/opposed-phase/fat/water images, T2-weighted imaging with and without fat suppression and diffusion-weighted imaging with corresponding ADC maps. Dynamic contrast-enhanced imaging was obtained after administration of gadoterate meglumine (0.1

mmol/kg, Dotarem<sup>®</sup>; Guerbet, Princeton, NJ, USA) at 1–2 mL/s followed by a saline flush, acquiring pre-contrast, arterial (35–40 s), portal venous (60–75 s), and delayed phase (3–5 min) images.

The prostate protocol consisted of high-resolution T2-weighted imaging in axial, sagittal, and coronal planes, diffusion-weighted imaging with corresponding ADC maps, and dynamic contrast-enhanced imaging following intravenous administration of gadobutrol (Gadavist, Bayer HealthCare) at a dose of 0.1 mmol/kg body weight at a rate of 2 mL/s, followed by a 20 mL saline flush.

The reference facility started incorporating deep learning (DL) reconstruction techniques in late 2021, while the optimized facility utilized DL reconstruction from its inception in March 2022.

### Data extraction and workflow metrics

Our analysis relied on two primary data sources: automated scanner logs provided by the vendor (Siemens Healthineers, Forchheim, Germany), which contained timestamps for all MRI scanner events, and electronic health records (EHR) exam data. These datasets were accurately matched by exam IDs and overlapping timestamps.

From this combined dataset, we extracted and evaluated several key workflow metrics (Fig. 1). The patient arrival to exam start time measured the interval between a patient's check-in at the imaging facility and the start of their examination. We also assessed the total process cycle, which encompassed the entire duration from the start of one exam to the beginning of the next. This cycle comprised three distinct components: positioning time, acquisition time, and table turnaround time. Positioning time reflects the essential patient positioning and preparation steps that occur on the scanner table itself in the scanner room. It is defined as the sum of two specific intervals: (1) the time between when the scanner first detects table activity (such as vertical table movement or docking) until the start of the first imaging sequence, and (2) the time between the end of the final imaging sequence until the scanner's last detection of table activity (such as undocking or table movement). Acquisition time represented the duration of active image acquisition, measured from the start of the first sequence to the end of the last. Table turnaround time captured the interval between the last event associated with one patient and the first event of the subsequent patient on the same scanner (i.e. vertical table movement, un-/docking table). To ensure data integrity and account for patient availability, we only calculated table turnaround time when the next patient arrived at least 10 min before the conclusion of the current exam.

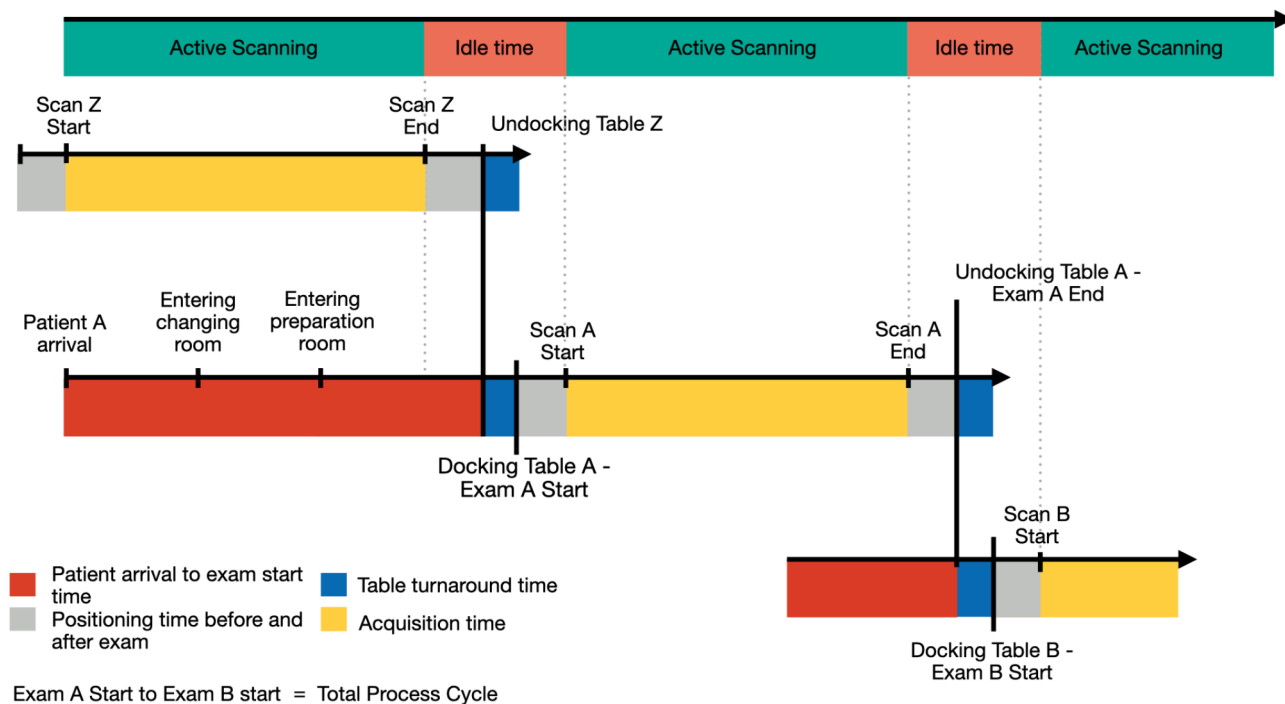


**Fig. 1.** Schematic diagram outlining the stages of the MRI examination process. The top row displays the scanner status, alternating between active scanning (green) and idle time (coral). The three timelines below demonstrate a sequence of patient examinations. The middle timeline follows Patient A's complete examination cycle: patient arrival to exam start time (red) begins when Patient A enters the facility and includes time in changing room and preparation bay; table turnaround time (blue) is defined as the interval between undocking Patient Z's table and docking Patient A's table; positioning time (gray) represents both the initial period between table docking and start of scanning, and the final period between last sequence and table undocking; acquisition time (yellow) captures the duration of active scanning. The bottom timeline shows the beginning of Patient B's examination as Patient A's concludes. The total process cycle is defined as the interval from the start of one examination to the start of the next (e.g., Exam A Start to Exam B Start).

While the scanner log files provided data for process cycle time, acquisition time, positioning time, and table turnaround time, we extracted patient arrival and scheduled exam times from the EHR.

### Statistical analysis

All calculations were performed using SPSS (Version 29.0.0.0, IBM Corp., Armonk, NY), and all graphics were generated using R Studio (Version 2024.04.2 + 764 Posit, PBC, Boston, MA). Descriptive statistics were conducted for patient characteristics and exam distribution across the imaging facilities and over time.

A three-way analysis of variance (ANOVA) was used to assess the impact of facility design, body region, and date (independent variables) on the key workflow metrics extracted from the scanner log (dependent variables). Estimated marginal means (EMM) and standard errors (SE), as well as the mode for table turnaround time, were reported. Post-hoc analysis using Bonferroni correction was conducted for pairwise multiple comparisons.

On-time performance was calculated for each facility type to compare the percentage of examinations starting within 5 min of the scheduled time. Chi-square tests were used to assess differences in categorical variables between the two facilities.

A 95% confidence interval was used, and  $p$ -values  $< 0.05$  were considered statistically significant.

### Declaration of AI and AI-assisted technologies in the writing process

During the preparation of this work the authors used “Claude 3.5 Sonnet AI Assistant. Anthropic, PBC” in order to improve the readability, language and quality of the writing. After using this service, the authors reviewed and edited the content as needed and take full responsibility for the content of the publication.

### Results

Between March 2022 and April 2024, a total of 2,723 MRI exams were analyzed across the two facilities. Over this 24-month period, 1,640 exams were performed at the optimized facility versus 1,083 at the reference facility, a 51.43% difference. These exams comprised 1,079 liver (694 at OF; 385 at RF) and 1,644 prostate (946 at OF; 698 at RF) scans. When accounting for the number of scanners (3 at OF, 1 at RF), OF's per-scanner throughput ranged from 35.3 to 90.0 exams per quarter, compared to RF's 41 to 209 exams per quarter. Patient demographics differed significantly between facilities, with RF patients being older on average (63 years,  $SE = 0.7$ ) compared to OF patients (60 years,  $SE = 0.4$ ,  $p < 0.001$ ). Overall, both facilities had a predominance of male patients (RF: 83.3%, OF: 80.3%), while for liver MRIs the distribution was nearly balanced (RF: 53.0% male, OF: 53.4% male).

### Punctuality and on-time performance

The mean time from patient arrival to the start of the exam was significantly shorter for patients in OF (28.7 min) compared to RF (37.7 min) ( $p < 0.001$ ). On-time performance was significantly higher for OF, with 79.4% of exams starting within 5 min of the scheduled appointment vs. 66.0% for RF ( $p < 0.001$ ). OF exams began an average of 7.8 min ( $SE = 0.7$ ) earlier than scheduled, while RF exams started 0.5 min ( $SE = 1.3$ ) earlier ( $p < 0.001$ ).

### Comparison and breakdown of total process cycle

The total process cycle, encompassing acquisition time, positioning time, and table turnaround time, was consistently shorter at OF. For liver exams, OF averaged 30.6 min compared to RF's 32.7 min, a 2.1-minute (6.4%) reduction ( $p < 0.01$ ). The difference was more pronounced for prostate exams, with OF averaging 32.5 min versus RF's 36.4 min, a 3.9-minute (10.7%) reduction ( $p < 0.001$ ) (Fig. 2).

Mean table turnaround time was significantly shorter at OF (4.6 min) compared to RF (8.3 min), resulting in a mean reduction of 3.7 min ( $p < 0.001$ ). For liver exams, OF achieved a mean reduction of 3 min (4.9 min at OF vs. 7.9 min at RF,  $p < 0.001$ ), while for prostate exams, the reduction was 4.4 min (4.2 min at OF vs. 8.6 min at RF,  $p < 0.001$ ). Regarding the distribution of table turnaround time, the most frequent (modal) turnaround time was 1 min for OF compared to 6 min for RF (Fig. 3). OF achieved a turnaround time of  $\leq 1$  min in 37.2% of exams versus 0.6% at RF ( $p < 0.001$ ), and  $\leq 3$  min in 61.3% of exams, compared to 3.5% at RF ( $p < 0.001$ ). The majority of RF exams (73.4%) had a turnaround between 4 and 10 min, while only 27.5% of OF exams fell into this range. RF had a higher proportion of exams with turnaround times  $> 10$  min (23.0%) compared to OF (11.3%).

Acquisition times showed minor differences between facilities with no significant difference for prostate exams. For liver exams, OF demonstrated a mean of 22.3 min compared to 21.4 min at RF ( $p < 0.05$ ). Prior to implementing DL sequences at the reference facility in late 2021, mean acquisition times for non-DL exams were 25.3 and 29.7 min for liver and prostate exams, respectively. During the study period, acquisition times of exams incorporating DL sequences at RF decreased to 21.2 and 25.3 min, representing reductions of 4.1 (16.2%) and 4.4 (14.8%) minutes. The optimized facility, using DL sequences from inception, achieved mean times of 22.3 and 25.5 min for liver and prostate exams. Compared to RF's pre-DL implementation, these represent reductions of 3.0 (11.9%) and 4.2 (14.1%) minutes for liver and prostate exams, respectively. All reductions were statistically significant ( $p < 0.001$ ).

Positioning times were equal between facilities for liver exams (3.4 min for both), and similar for prostate exams (2.8 min at OF vs. 2.5 min at RF ( $p < 0.05$ )). A comprehensive summary of all workflow metrics is presented in Table 1.

### Discussion

Our study offers a unique comparison between two high-performance MRI facilities: a reference facility (RF) specializing in abdominal imaging and a newly designed optimized facility (OF) that incorporates innovative architectural and operational strategies. Despite the RF's already efficient workflow, the OF demonstrated significant enhancements across several key performance metrics. The introduction of novel design elements and

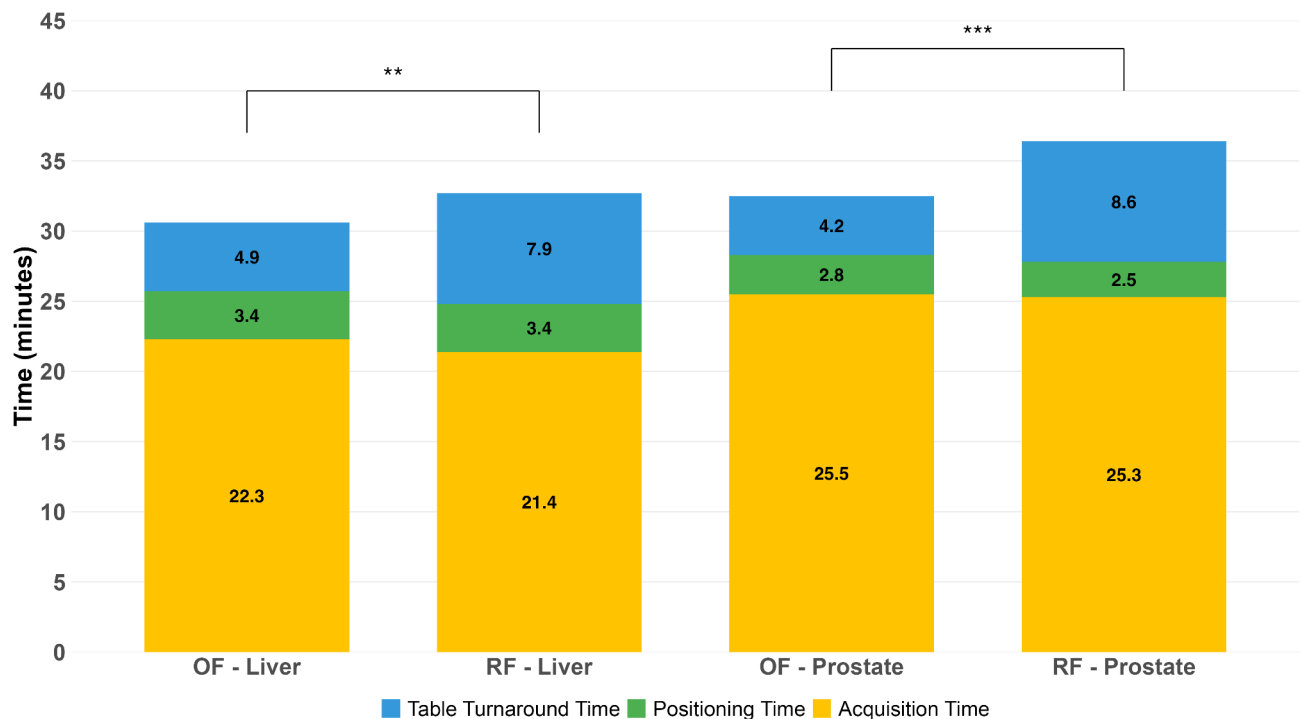


**Fig. 2.** Comparison of the total process cycle for liver and prostate exams at the optimized (OF) and reference facilities (RF) from March 2022 to April 2024. The graph highlights the shorter table turnaround times across all exam types at OF, while other metrics remain comparable between facilities. Asterisks indicate statistically significant differences in the total process cycle between OF and RF (\*\* $p < 0.01$ , \*\*\* $p < 0.001$ ).

workflow optimizations at the OF led to reduced total process cycle times, significantly shorter table turnaround times, and improved on-time performance. Notably, both facilities benefited from the implementation of deep learning-based image reconstruction techniques, significantly reducing acquisition times.

In the context of workflow optimization in MRI, several previous studies have demonstrated significant potential for efficiency improvements. Beker et al. conducted a comprehensive, prospective analysis of MRI workflow efficiency, examining 305 examinations across all body regions over a two-week period<sup>8</sup>. Their findings revealed that only 38% of the total patient experience constituted value-added time, highlighting substantial room for workflow optimization. Our study builds upon these insights but focuses specifically on abdominal MRI examinations over a 25-month period (March 2022 to April 2024) and with a larger patient cohort (2,723 exams), providing more robust data for this particular subspecialty. Other architectural design studies, like Recht et al., demonstrated mean time savings of 5.5 min per examination through the use of dockable tables<sup>9</sup>. While the latter focused primarily on table turnaround time, our investigation provides a more comprehensive evaluation by examining multiple workflow components throughout the examination process.

In our study, the total process cycle was consistently shorter at OF for both liver and prostate exams with mean reductions of 2.1-minutes (6.4%) for liver exams and 3.9-minutes (10.7%) for prostate exams ( $p < 0.001$ ). These reductions, while modest, are significant given that RF is already a highly efficient facility. Based on our operational hours (6:30 AM to 10:00 PM, 930 min), OF could perform 29.5 exam cycles per scanner daily compared to RF's 26.9, representing a 9.6% increase in daily capacity or 2–3 additional exams per scanner.

The most striking difference between the two facilities was observed in table turnaround times. OF achieved mean turnaround times of 4.6 min versus RF's 8.3 min - a 3.7-minute reduction. This improvement is attributable to OF's design features: dockable tables and dedicated preparation bays enable concurrent patient preparation during active scanning, while eliminating patient walking time to and from the scanner room. Remarkably, over 37% of exams at the OF achieved a turnaround time of  $\leq 1$  min, compared to just 0.6% at the RF. This rapid turnaround, achieved in more than a third of cases, likely reflects optimal conditions, including the absence of unexpected delays, adequate technician availability, and the timely completion of prior exams. Under optimal conditions with consistent 1-minute turnarounds, OF could theoretically perform 33.3 exam cycles per scanner daily - a 23.8% efficiency gain over RF, equivalent to 6–7 additional exams per scanner per day.

As anticipated, acquisition times showed minor differences between the facilities, with the OF exhibiting slightly longer times for liver exams and no significant difference for prostate exams. This finding is particularly noteworthy considering that the RF is a specialized abdominal MR imaging center known for its high throughput and highly optimized scanning processes. The marginally longer acquisition times at the OF may be attributed to the ongoing testing of new sequences and of deep learning applications, underscoring its role as an innovative facility. Despite these slightly longer acquisition times at the OF, the introduction of DL sequences at both

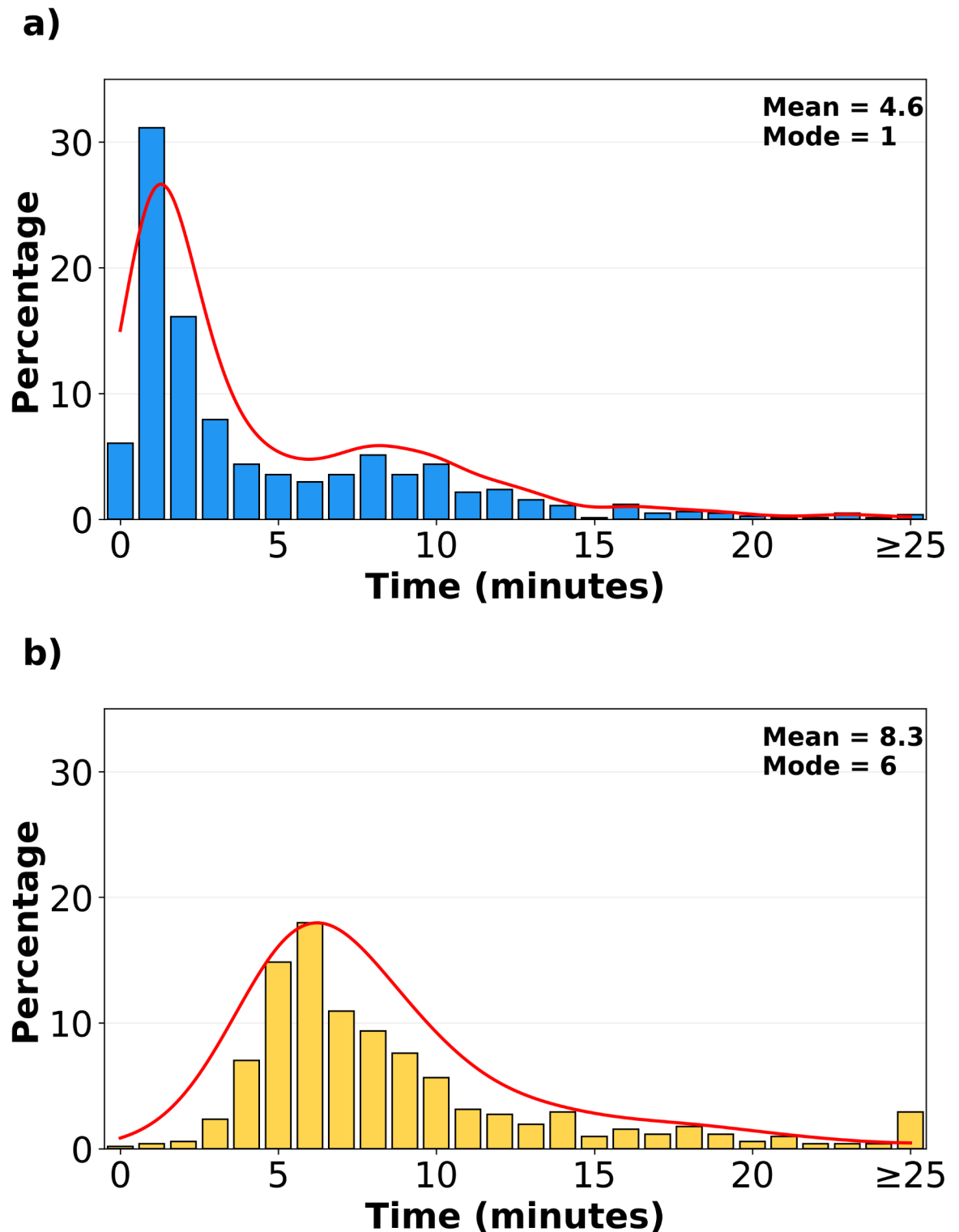


**Fig. 3.** Distribution of table turnaround time (TTT) for the optimized (OF) and reference facility (RF). OF's histogram reveals a strong right skew, with a pronounced peak at 1 min (mode), and the majority of the patients (61.3%) swapped within  $\leq 3$  min. In contrast RF's histogram exhibits a more symmetrical distribution compared to the OF, with a central peak at 6 min (mode) and the majority of patients (73.4%) swapped within 4–10 min. The red line shows the kernel density estimation of the distribution.



Body Region	Metric	Optimized MRI Facility	Reference MRI Facility	OF vs. RF (Difference, <i>p</i> -value)
Overall		<i>n</i> = 1640	<i>n</i> = 1083	
	Age (years)	60 (0.4)	63 (0.7)	<i>p</i> < 0.001
	Male	80.3%	83.3%	<i>p</i> < 0.05
	Patient Time Slots	30	45	-
	Patient Arrival to Exam Start Time	28.7 (0.5)	37.7 (1.0)	-9.0 (-23.9%), <i>p</i> < 0.001
Liver		<i>n</i> = 694	<i>n</i> = 385	
	Male	53.4%	53%	<i>p</i> = 0.989
	Acquisition Time	22.3 (0.2)	21.4 (0.3)	+ 0.9 (+ 4.2%), <i>p</i> < 0.05
	Positioning Time	3.4 (0.1)	3.4 (0.1)	0.0 (0.0%), <i>p</i> = 0.999
	Table Turnaround Time	4.9 (0.3)	7.9 (0.6)	-3.0 (-38%), <i>p</i> < 0.001
	Total Process Cycle	30.6 (0.3)	32.7 (0.7)	-2.1 (-6.4%), <i>p</i> < 0.01
Prostate		<i>n</i> = 946	<i>n</i> = 698	
	Acquisition Time	25.5 (0.2)	25.3 (0.3)	+ 0.2 (+ 0.8%), <i>p</i> = 0.619
	Positioning Time	2.8 (0.1)	2.5 (0.1)	+ 0.3 (+ 12%), <i>p</i> < 0.05
	Table Turnaround Time	4.2 (0.3)	8.6 (0.6)	-4.4 (-51.2%), <i>p</i> < 0.001
	Total Process Cycle	32.5 (0.3)	36.4 (0.6)	-3.9 (-10.7%), <i>p</i> < 0.001

**Table 1.** Patient characteristics and workflow metrics. Differences in patient demographics and key workflow metrics for liver and prostate exams at both facilities (OF = Optimized Facility, RF = Reference Facility). All time values are presented in minutes as mean (SE).

facilities resulted in significant reductions in acquisition times compared to pre-DL periods, underscoring the potential of this technology to enhance MRI efficiency.

OF demonstrated superior on-time performance with a higher proportion of starting within 5 min of the scheduled time OF started compared to RF. The time from patient arrival to exam start was significantly shorter at OF (28.7 min) compared to RF (37.7 min). This interval represents the time spent in the waiting area, changing room and preparation bay. The reduction in this time at OF can be mainly attributed to the parallel preparation processing of the patient on the dockable table in the preparation bay.

Our study has several important limitations that should be considered when interpreting the results. First, our primary data was extracted directly from MRI scanner logs, which may not fully capture all aspects of the patient experience and the overall workflow. This limitation is particularly relevant in our analysis of the time from patient arrival to exam start. While we observed a significant reduction in this metric at the OF compared to the RF, the scanner logs do not provide granular details about specific pre-exam activities, such as patient registration, changing, or preparation in the dedicated bays. As a result, we are unable to precisely quantify the time savings for each step of the pre-exam process or definitively attribute these reductions to specific design elements or operational changes at the OF.

Another significant limitation of our study design is the inherent difference in scanner availability between the OF and RF. With its three scanners, the OF has an intrinsic advantage over the single-scanner RF in terms of flexibility and patient management. This disparity allows the OF to potentially switch patients between scanners if one becomes available earlier, thereby increasing overall productivity. This setup difference likely contributes to the superior on-time performance and shorter patient wait times observed at the OF.

Lastly, our study does not include a comprehensive cost-effectiveness analysis of the new facility design and operational modifications. Although we demonstrate enhanced efficiency, we cannot assess the economic viability or return on investment of implementing similar changes in other settings. However, our research group is currently actively conducting a detailed time-driven activity-based costing (TDABC) study comparing the economic implications of different MRI facility designs in our institution.

In conclusion, our study demonstrates that innovative architectural and operational strategies in MRI facility design can significantly improve workflow efficiency, even compared to an already highly efficient reference facility. Significant reductions in total process cycle times were achieved through shorter table turnaround times, along with superior on-time performance and shorter patient wait times. While our study focused on abdominal imaging, these principles of parallel processing and optimized patient flow could be applicable across other MRI applications and healthcare settings. These findings suggest that comprehensive redesign approaches, incorporating features such as dockable tables and dedicated preparation bays, could effectively meet the growing demand for MRI services.

Data availability

The datasets used and analyzed during the current study are available from the corresponding author on reasonable request.

Received: 8 October 2024; Accepted: 17 March 2025  
Published online: 30 March 2025

## References

1. Hofmann, B., Haug, E. S., Andersen, E. R. & Kjelle, E. Increased magnetic resonance imaging in prostate cancer management—What are the outcomes? *J. Eval. Clin. Pract.* **29** (6), 893–902. <https://doi.org/10.1111/jep.13791> (2023).
2. Gaffney, C. D. et al. Increasing utilization of MRI before prostate biopsy in black and Non-Black men: an analysis of the SEER-Medicare cohort. *AJR Am. J. Roentgenol.* **217** (2), 389–394. <https://doi.org/10.2214/AJR.20.23462> (2021).
3. Taouli, B., Ehman, R. L. & Reeder, S. B. Advanced MRI methods for assessment of chronic liver disease. *AJR Am. J. Roentgenol.* **193** (1), 14–27. <https://doi.org/10.2214/AJR.09.2601> (2009).
4. Ringe, K. I. et al. Abbreviated MRI protocols in the abdomen and pelvis. *J. Magn. Reson. Imaging.* **59** (1), 58–69. <https://doi.org/10.1002/jmri.28764> (2024).
5. Yoon, J. H., Nickel, M. D., Peeters, J. M. & Lee, J. M. Rapid imaging: recent advances in abdominal MRI for reducing acquisition time and its clinical applications. *Korean J. Radiol.* **20** (12), 1597–1615. <https://doi.org/10.3348/kjr.2018.0931> (2019).
6. Hamilton, J., Franson, D. & Seiberlich, N. Recent advances in parallel imaging for MRI. *Prog. Nucl. Magn. Reson. Spectrosc.* **101**, 71–95. <https://doi.org/10.1016/j.pnmrs.2017.04.002> (2017).
7. Afat, S. et al. Analysis of a deep Learning-Based superresolution algorithm tailored to partial fourier gradient echo sequences of the abdomen at 1.5 T: reduction of Breath-Hold time and improvement of image quality. *Invest. Radiol.* **57** (3), 157–162. <https://doi.org/10.1097/RLI.0000000000000825> (2022).
8. Beker, K. et al. Prospective analysis of performance, efficiency, and patient throughput. *AJR Am. J. Roentgenol.* **209** (4), 836–844. <https://doi.org/10.2214/AJR.16.17698> (2017).
9. Recht, M. P. et al. Optimization of MRI turnaround times through the use of dockable tables and innovative architectural design strategies. *AJR Am. J. Roentgenol.* **212** (4), 855–858. <https://doi.org/10.2214/AJR.18.20459> (2019).
10. Lang, M. et al. Improving workflow efficiency at an outpatient MRI imaging facility: A case study. *J. Am. Coll. Radiol.* **20**, S1546–1440(24)00531–3. <https://doi.org/10.1016/j.jacr.2024.06.007> (2024).

## Acknowledgements

We acknowledge the support from the Medical Analytics Group, Massachusetts General Hospital, and Harvard Medical School, who provided the MRI scanner log and EHR data.

## Author contributions

All authors contributed to the study conception and design. Material preparation, data collection and analysis were performed by A.S., W.L., S.H., A.H., B.W. and M.W. M.W. and A.H. performed statistical analysis of the data. The first draft of the manuscript was written by A.H. All authors contributed to manuscript revision for important intellectual content. All authors read and approved the final manuscript.

## Declarations

## Competing interests

W.L., B.C. and M.W. are employees at Siemens Medical Solutions. S. H. is a consultant for Siemens Healthineers. This study was supported by a research grant from Siemens Healthineers. The remaining authors have no competing interest to declare.

## Additional information

**Correspondence** and requests for materials should be addressed to O.A.C.

**Reprints and permissions information** is available at [www.nature.com/reprints](http://www.nature.com/reprints).

**Publisher's note** Springer Nature remains neutral with regard to jurisdictional claims in published maps and institutional affiliations.

**Open Access** This article is licensed under a Creative Commons Attribution-NonCommercial-NoDerivatives 4.0 International License, which permits any non-commercial use, sharing, distribution and reproduction in any medium or format, as long as you give appropriate credit to the original author(s) and the source, provide a link to the Creative Commons licence, and indicate if you modified the licensed material. You do not have permission under this licence to share adapted material derived from this article or parts of it. The images or other third party material in this article are included in the article's Creative Commons licence, unless indicated otherwise in a credit line to the material. If material is not included in the article's Creative Commons licence and your intended use is not permitted by statutory regulation or exceeds the permitted use, you will need to obtain permission directly from the copyright holder. To view a copy of this licence, visit <http://creativecommons.org/licenses/by-nc-nd/4.0/>.

© The Author(s) 2025